

Capacitance Sensitivity Calculation for Interconnects by Adjoint Field Technique

Yu Bi¹, N.P. van der Meijs¹, Daniel Ioan²

¹Circuits and Systems, Delft University of Technology

²Numerical Methods Laboratory, Politechnica University of Bucharest
y.bi@tudelft.nl; nick@cobalt.et.tudelft.nl; daniel@lmn.pub.ro

Abstract

This paper presents a new, efficient algorithm for capacitance sensitivity calculation w.r.t. geometric variations due to process imperfection of interconnects. Sensitivity calculation can be a very important step in variation-aware interconnect analysis. The algorithm is based on the Adjoint Field Technique (AFT) derived from an application of Tellegen's theorem for the electrostatic (ES) field. The algorithm relies on manipulating the intermediate data of a standard (without considering variations) capacitance extraction. Thus no additional costly computations are required, which makes the algorithm very efficient. The algorithm has been verified for 2D structures while the generalization for 3D structures is straightforward.

Introduction

The on-going reduction of feature size goes together with an increase of manufacturing variability, of which the impact on the interconnect performance has become extremely important. In particular, capacitance extraction considering process variations has been gaining more and more attention. A popular approach is to use sensitivity models with the final capacitance as a function of geometry variations [1] [2] and [3].

A key requirement for this type of approach is the ability to calculate the sensitivity coefficients accurately and efficiently. Different techniques have been utilized to do that: numerical differencing in [2] and analytic differencing of empirical capacitance models in [1] [3]. In this paper, we propose a new technique of capacitance sensitivity calculation by the Adjoint Field Technique (AFT) which is in fact an application of Tellegen's theorem [4].

The remainder of this paper is organized as follows: We start with an introduction of AFT for the ES field derived from Tellegen's theorem; then a detailed analysis of our algorithm is given, followed by an illustrative example. Next, experiments and results will be shown to verify the algorithm and the conclusion is given at the end.

Adjoint Field Technique/Tellegen's Theorem

Consider a circuit network with m ports and n internal branches (excluding the port branches). A combination of Kirchhoff's current law and voltage law applied to the network can lead to

$$\mathbf{I}_m^T \mathbf{V}_m = \mathbf{I}_n^T \mathbf{V}_n \quad (1)$$

where \mathbf{I}_m and \mathbf{V}_m are currents and voltages at the ports

while \mathbf{I}_n and \mathbf{V}_n are on the branches in the interior of the network. This is called the "actual-power theorem" [5] which is consistent with the principle of energy conservation. While the "actual-power theorem" (1) being applied for one circuit network, the "quasi-power theorem", well-known as "Tellegen's theorem" [4] [5], gives a similar equation for two networks with the same topology:

$$\mathbf{I}_m^T \hat{\mathbf{V}}_m = \mathbf{I}_n^T \hat{\mathbf{V}}_n \quad (2)$$

The two networks are usually referred to as the original network and the adjoint/auxiliary network. To distinguish them, we use a notation " $\hat{\cdot}$ " for the adjoint network quantities throughout this paper.

Originated from circuit networks, Tellegen's theorem has been generalized to the electromagnetic fields [6] [7]. In this paper we will show another application of Tellegen's theorem for the ES field.

Assume that there are N conductors in the uncharged open space where the absolute zero potential is considered at infinity. We know the ES energy is

$$U = \frac{1}{2} \sum_{i=1}^N V_i q_i \quad (3)$$

where V_i is the absolute ES potential and q_i is the total charge of the i^{th} conductor ($i = 1, \dots, N$) [8].

We also know that in the ES field, the stored electric energy for a configuration of static charges is the amount of work required to assemble such a configuration, which is given as [8] [9]

$$W = \frac{1}{2} \int_{\Omega} \mathbf{E} \mathbf{D} d\Omega. \quad (4)$$

Apparently (3) and (4) are two different forms of the expression of the ES energy, which means $U = W$. This can be written as

$$(\mathbf{V}, \mathbf{q}) = \langle \mathbf{E}, \mathbf{D} \rangle \quad (5)$$

where $(\mathbf{V}, \mathbf{q}) = \mathbf{V}^T \cdot \mathbf{q}$ and $\langle \mathbf{E}, \mathbf{D} \rangle = \int_{\Omega} \mathbf{E} \mathbf{D} d\Omega$. Equation (5) shows the energy conservation for the ES field and analogically to (1) and (2), we can, without proof, obtain Tellegen's theorem for the ES field expressed as

$$(\hat{\mathbf{V}}, \mathbf{q}) = \langle \hat{\mathbf{E}}, \mathbf{D} \rangle \quad (6)$$

or

$$(\mathbf{V}, \hat{\mathbf{q}}) = \langle \mathbf{E}, \hat{\mathbf{D}} \rangle. \quad (7)$$

If \mathbf{q} in the original network is changed by $\Delta \mathbf{q}$, based on

This work is supported by the European project CHAMELEON RF (IST-027378).

the linearity of the inner product, (6) can lead us to

$$(\hat{\mathbf{V}}, \Delta \mathbf{q}) = \langle \hat{\mathbf{E}}, \Delta \mathbf{D} \rangle. \quad (8)$$

Similarly, we can derive from (7) that

$$(\Delta \mathbf{V}, \hat{\mathbf{q}}) = \langle \Delta \mathbf{E}, \hat{\mathbf{D}} \rangle. \quad (9)$$

Subtracting (8) from (9) gives us

$$(\Delta \mathbf{V}, \hat{\mathbf{q}}) - (\hat{\mathbf{V}}, \Delta \mathbf{q}) = \langle \Delta \mathbf{E}, \hat{\mathbf{D}} \rangle - \langle \hat{\mathbf{E}}, \Delta \mathbf{D} \rangle \quad (10)$$

It is well-known that $\mathbf{q} = \mathbf{C}\mathbf{V}$. Considering the fact that $\Delta \mathbf{V} = 0$ in our sensitivity study because the excitation voltages are not influenced by geometric variations, the change in \mathbf{q} due to the variation in p can be written as

$$\Delta \mathbf{q} = (\Delta \mathbf{C})\mathbf{V} + \mathbf{C}(\Delta \mathbf{V}) = (\Delta \mathbf{C})\mathbf{V} \quad (11)$$

In linear isotropic media we have $\mathbf{D} = \epsilon \mathbf{E}$ and $\hat{\mathbf{D}} = \epsilon \hat{\mathbf{E}}$. Thus using $\Delta \mathbf{V} = 0$, the substitution of (11) in (10) results in

$$\begin{aligned} -(\hat{\mathbf{V}}, (\Delta \mathbf{C})\mathbf{V}) &= \langle \Delta \mathbf{E}, \epsilon \hat{\mathbf{E}} \rangle - \langle \hat{\mathbf{E}}, \Delta(\epsilon \mathbf{E}) \rangle \\ &= \langle \Delta \mathbf{E}, \epsilon \hat{\mathbf{E}} \rangle - \langle \hat{\mathbf{E}}, \epsilon \Delta \mathbf{E} \rangle - \langle \hat{\mathbf{E}}, \mathbf{E} \Delta \epsilon \rangle \\ &= - \langle \hat{\mathbf{E}}, \mathbf{E} \Delta \epsilon \rangle \end{aligned}$$

Consequently,

$$(\hat{\mathbf{V}}, (\Delta \mathbf{C})\mathbf{V}) = \langle (\Delta \epsilon) \mathbf{E}, \hat{\mathbf{E}} \rangle \quad (12)$$

This is the main result of AFT for our capacitance sensitivity calculation from a theoretical point of view. Next we will show how to develop (12) into an applicable algorithm.

Algorithm Analysis

To compute the sensitivity of a particular capacitance w.r.t. a certain geometric parameter, e.g., $\frac{\partial C_{ij}}{\partial p}$, we should first select the specific capacitance C_{ij} . For this purpose, let's look at the left-hand side of Equation (12): $(\hat{\mathbf{V}}, (\Delta \mathbf{C})\mathbf{V})$. Assume that there are N conductors in the system and we have

$$\begin{aligned} (\hat{\mathbf{V}}, (\Delta \mathbf{C})\mathbf{V}) &= \\ \begin{pmatrix} \hat{V}_1 \\ \vdots \\ \hat{V}_i \\ \vdots \\ \hat{V}_N \end{pmatrix}^T & \begin{pmatrix} \Delta C_{11} & \cdots & \Delta C_{1j} & \cdots & \Delta C_{1N} \\ \vdots & & \vdots & & \vdots \\ \Delta C_{i1} & \cdots & \Delta C_{ij} & \cdots & \Delta C_{iN} \\ \vdots & & \vdots & & \vdots \\ \Delta C_{N1} & \cdots & \Delta C_{Nj} & \cdots & \Delta C_{NN} \end{pmatrix} \begin{pmatrix} V_1 \\ \vdots \\ V_j \\ \vdots \\ V_N \end{pmatrix} \end{aligned}$$

If we want to calculate ΔC_{ij} , we need to define the excitation voltages of the original system as

$$V_j = V_0 = 1 \quad \text{and} \quad V_k = 0 \quad \forall k \neq j; \quad (13)$$

and the excitation voltages of the adjoint system as

$$\hat{V}_i = V_0 = 1 \quad \text{and} \quad \hat{V}_k = 0 \quad \forall k \neq i. \quad (14)$$

Therefore,

$$(\hat{\mathbf{V}}_i, (\Delta \mathbf{C})\mathbf{V}_j) = (\Delta C_{ij}) V_0^2 = \Delta C_{ij} \quad (15)$$

where \mathbf{V}_j is a vector whose elements are under condition (13) and $\hat{\mathbf{V}}_i$ is a vector whose elements are under condition (14).

Now we consider a more general situation where each conductor is discretized so that the Boundary Element Method (BEM) can be applied. For simplicity reasons, we use the piecewise constant (PWC) shape function for the rest of this paper. Each conductor is uniformly discretized with n panels which leads to a total number of $m = n \times N$ panels in series in the system. For example, conductor j has panels numbered from $(j-1)n+1$ to jn . The discretization is identical for the adjoint system.

We then use incidence matrices \mathbf{A} (for the original system) and $\hat{\mathbf{A}}$ (for the adjoint system) to relate the panels to the applied voltage ($\phi \in \{1, 0\}$), which further, as will be explained later, determine the specific capacitance to be calculated.

For example, we want to calculate ΔC_{ij} . Based on (13), (14) and (15), $1(V)$ is applied to the j^{th} conductor and $0(V)$ to the others for the original system while for the adjoint system $1(V)$ to the i^{th} conductor and $0(V)$ to the others. Considering there are n panels on each conductor and making use of the incidence matrices \mathbf{A} and $\hat{\mathbf{A}}$, we arrive at a generalization of (13) and (14):

$$\begin{aligned} \mathbf{V}_j &= \mathbf{A}_j \phi \\ &= \begin{pmatrix} \text{zeros}(1, (j-1)n)^T & \text{ones}(1, (j-1)n)^T \\ \text{ones}(1, n)^T & \text{zeros}(1, n)^T \\ \text{zeros}(1, (N-j)n)^T & \text{ones}(1, (N-j)n)^T \end{pmatrix} \begin{pmatrix} 1 \\ 0 \end{pmatrix} \end{aligned} \quad (16)$$

$$\begin{aligned} \hat{\mathbf{V}}_i &= \hat{\mathbf{A}}_i \phi \\ &= \begin{pmatrix} \text{zeros}(1, (i-1)n)^T & \text{ones}(1, (i-1)n)^T \\ \text{ones}(1, n)^T & \text{zeros}(1, n)^T \\ \text{zeros}(1, (N-i)n)^T & \text{ones}(1, (N-i)n)^T \end{pmatrix} \begin{pmatrix} 1 \\ 0 \end{pmatrix} \end{aligned} \quad (17)$$

where we use the Matlab notation to describe \mathbf{A}_j and $\hat{\mathbf{A}}_i$. Substituting (16) and (17) in (15), we obtain

$$\Delta C_{ij} = (\hat{\mathbf{V}}_i, (\Delta \mathbf{C})\mathbf{V}_j) = \hat{\mathbf{V}}_i^T \cdot (\Delta \mathbf{C})\mathbf{V}_j = \phi^T \hat{\mathbf{A}}_i^T (\Delta \mathbf{c}) \mathbf{A}_j \phi$$

where \mathbf{c} is the so-called partial capacitance matrix (c -matrix) [10]. The elements of c -matrix are in fact the capacitances associated to the BEM discretization panels before their association to conductors. Note that there are in total m panels in the system, thus $\Delta \mathbf{c}$ (the variation in partial capacitances due to Δp) is an $m \times m$ matrix. The choice of incidence matrices \mathbf{A} and $\hat{\mathbf{A}}$ for the original and the adjoint systems respectively depends on the particular capacitance (ΔC_{ij}) we want to calculate.

Next, let's look at the right-hand side of Equation (12): $\langle (\Delta \epsilon) \mathbf{E}, \hat{\mathbf{E}} \rangle$, where $\Delta \epsilon$ is the variation in the permittivity due to the variation in p (Δp).

By combining (12) and (15), we can derive that

$$\frac{\partial C_{ij}}{\partial p} = \int_{\Omega} \left(\frac{\partial \epsilon}{\partial p} \right) \mathbf{E} \hat{\mathbf{E}} d\Omega \quad (18)$$

where by definition

$$\frac{\partial C_{ij}}{\partial p} = \lim_{\Delta p \rightarrow 0} \frac{\Delta C_{ij}}{\Delta p}.$$

There are two different cases depending on how the surface of the conductor varies:

1. The surface of the conductor expands outwards into the air. As we can see in Figure 1(a), the shadow area is where ϵ is changed. Specifically, the ϵ in the shadow area varies from ϵ_0 ($\epsilon_{air} = \epsilon_0$ in the air) to 0 ($\epsilon_{metal} \approx 0$ in the metal) so ϵ is changed by a value of

$$\Delta\epsilon = 0 - \epsilon_0 = -\epsilon_0. \quad (19)$$

2. The opposite situation is that the surface shrinks (Figure 1(b)) and the ϵ in the shadow area varies from 0 (in the metal) to ϵ_0 (in the air):

$$\Delta\epsilon = \epsilon_0 - 0 = \epsilon_0. \quad (20)$$

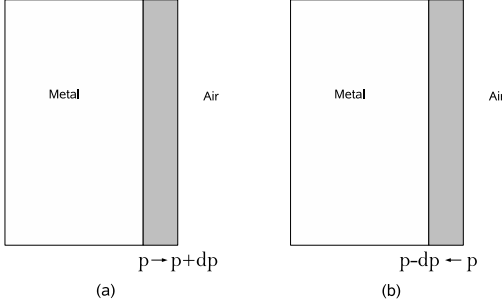


Figure 1: Schematics for the changes of ϵ .

Since the variation of the permittivity due to Δp only happens on the corresponding surface s_p , which is moved due to Δp , we have

$$d\Omega = \Delta p ds$$

where $d\Omega$ is basically the shadow area in Figure 1(a)/(b). Therefore the sensitivity (18) can be rewritten as,

$$\frac{\partial C_{ij}}{\partial p} = \int_{s_p} \lim_{\Delta p \rightarrow 0} \left(\frac{\Delta\epsilon}{\Delta p} \right) \mathbf{E} \hat{\mathbf{E}} \Delta p ds = \Delta\epsilon \int_{s_p} \mathbf{E} \hat{\mathbf{E}} ds \quad (21)$$

When the BEM is applied, \mathbf{E} is a piecewise constant quantity on the set of panels. Hence, the integration over s_p becomes a summation. When also using $\mathbf{D} = \epsilon \mathbf{E}$, we get

$$\frac{\partial C_{ij}}{\partial p} = \Delta\epsilon \int_{s_p} \mathbf{E} \hat{\mathbf{E}} ds = \Delta\epsilon \sum_{k \in s_p} E_k \hat{E}_k a_k = \frac{1}{\Delta\epsilon} \sum_{k \in s_p} D_k \hat{D}_k a_k \quad (22)$$

where a_k is the corresponding area of the k^{th} panel on the surface (s_p). With Gauss law $\nabla \cdot \mathbf{D} = \rho$ (where ρ is the charge density) applied to the conductor surfaces, (22) can be written

$$\frac{\partial C_{ij}}{\partial p} = \frac{1}{\Delta\epsilon} \sum_{k \in s_p} \rho_k \hat{\rho}_k a_k. \quad (23)$$

For a panel k ($k \in \{1, \dots, m\}$), since PWC is used for the BEM, the charge density ρ_k can be related to the charge q_k with the corresponding area a_k as $q_k = \rho_k a_k$, which leads to

$$\frac{\partial C_{ij}}{\partial p} = \frac{1}{\Delta\epsilon} \sum_{k \in s_p} q_k \hat{q}_k / a_k. \quad (24)$$

Based on (16) we have

$$\begin{aligned} \mathbf{q} &= \mathbf{C} \mathbf{V}_j = \mathbf{c} \mathbf{A}_j \phi \\ &= \begin{pmatrix} c_{1,(j-1)n+1} + c_{1,(j-1)n+2} + \dots + c_{1,jn} \\ c_{2,(j-1)n+1} + c_{2,(j-1)n+2} + \dots + c_{2,jn} \\ \vdots \\ c_{m,(j-1)n+1} + c_{m,(j-1)n+2} + \dots + c_{m,jn} \end{pmatrix} \\ &= \begin{pmatrix} \sum_{a=(j-1)n+1}^{jn} c_{1,a} \\ \sum_{a=(j-1)n+1}^{jn} c_{2,a} \\ \vdots \\ \sum_{a=(j-1)n+1}^{jn} c_{m,a} \end{pmatrix} \end{aligned}$$

Therefore

$$q_k = \sum_{a=(j-1)n+1}^{jn} c_{k,a}, \quad (25)$$

Similarly, based on (17) we have

$$\hat{\mathbf{q}} = \mathbf{C} \hat{\mathbf{V}}_i = \hat{\mathbf{c}} \hat{\mathbf{A}}_i \phi = \begin{pmatrix} \sum_{b=(i-1)n+1}^{in} c_{1,b} \\ \sum_{b=(i-1)n+1}^{in} c_{2,b} \\ \vdots \\ \sum_{b=(i-1)n+1}^{in} c_{m,b} \end{pmatrix} \quad (26)$$

and

$$\hat{q}_k = \sum_{b=(i-1)n+1}^{in} c_{k,b}. \quad (27)$$

The substitution of (25) and (27) in (24) gives us the final equation which will be used for the calculation of capacitance sensitivities:

$$\frac{\partial C_{ij}}{\partial p} = \frac{1}{\Delta\epsilon} \sum_{k \in s_p} \left(\sum_{a=(j-1)n+1}^{jn} c_{k,a} \right) \left(\sum_{b=(i-1)n+1}^{in} c_{k,b} \right) / a_k. \quad (28)$$

The development above actually presents the sensitivity in terms of partial capacitances, which can be extracted by the BEM-based layout-to-circuit extractor SPACE [11]. In the next section, we will use an example to illustrate the algorithm.

Illustrative Example

This is a system with two conductors ($N = 2$) as shown in Figure 2(a). In order to make the explanation clear and easy to understand, we assume that there are 2 panels on every surface and therefore $n = 8$ panels on each conductor. The system has thus altogether $m = n \times N = 16$ panels. The geometry parameter p is the width of conductor 1 and the affected surface s_p consists of panels nr.7 and 8.

According to (28), the sensitivity of the mutual capacitance (C_{21}) between conductor 1 and 2 w.r.t. p can be calculated as (Figure 2(b)),

$$\frac{\partial C_{21}}{\partial p} = \frac{1}{\Delta\epsilon} \left[\left(\sum_{a=1}^8 c_{7,a} \right) \left(\sum_{b=9}^{16} c_{7,b} \right) / a_7 + \left(\sum_{a=1}^8 c_{8,a} \right) \left(\sum_{b=9}^{16} c_{8,b} \right) / a_8 \right].$$

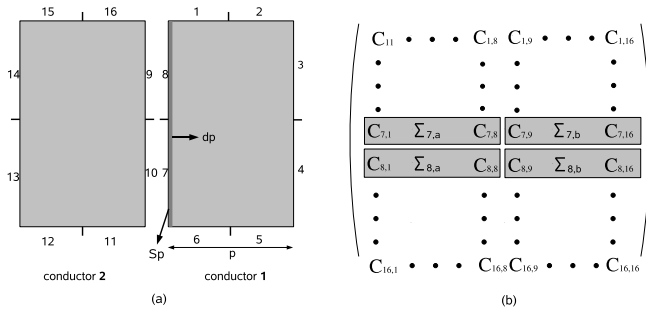


Figure 2: The system schematic (a) and the partial c -matrix (b) in the illustrative example.

Experiments and Results

In this section, two experiments will be shown to verify the accuracy of the algorithm described above. Again, we assume a system with two conductors for simplicity reasons (the schematic is the same as Figure 2(a)), but this is not a restriction of the method. In the first experiment, the distance between these two conductors (d) is taken as the geometric parameter. The widths of the conductors are $2\mu\text{m}$ and the heights are $3\mu\text{m}$. The total number of panels is 500. The main steps of the experiment are as follows:

1. Use the BEM to compute C as a function of d , resulting in $C_{BEM}(d)$.
2. Fit $C_{BEM}(d)$ with appropriate polynomial approximations. In this experiment, $1/d$ is taken as the variable of the polynomial and 2^{nd} order expansion of C is utilized:

$$C_{\text{approx.}}(d) = m_0 + m_1 \frac{1}{d} + m_2 \left(\frac{1}{d}\right)^2.$$

To achieve a high accuracy, the approximation is further divided into several subsections (i.e., three subsections in this case).

3. Use the polynomial fit above to compute the sensitivity by calculating the derivatives of the approximated capacitance w.r.t. d , resulting in $\frac{\partial C}{\partial d}^n$ (where the notation “ n ” represents for the numerical differencing method), which is considered as the reference of the sensitivity computed by the AFT method ($\frac{\partial C}{\partial d}^A$).
4. Compute the sensitivity using (28), and compare the result $\frac{\partial C}{\partial d}^A$ with $\frac{\partial C}{\partial d}^n$.

Figure 3 shows $\frac{\partial C}{\partial d}^n$ and $\frac{\partial C}{\partial d}^A$ w.r.t. d in the range of $0.5\mu\text{m} - 2\mu\text{m}$. The sensitivity calculated by AFT agrees well with $\frac{\partial C}{\partial d}^n$, which is taken as the reference. Table 1 shows the average and the maximum differences between them while the distance ranges from $0.5\mu\text{m}$ up to $12\mu\text{m}$ divided into three subsections.

Distance(μm)	Average Deviation	Max. Deviation
0.5 - 2	1.74%	2.99%
2 - 6	2.82%	4.76%
6 - 12	3.82%	4.93%

Table 1: Comparison between $\frac{\partial C}{\partial d}^A$ and $\frac{\partial C}{\partial d}^n$

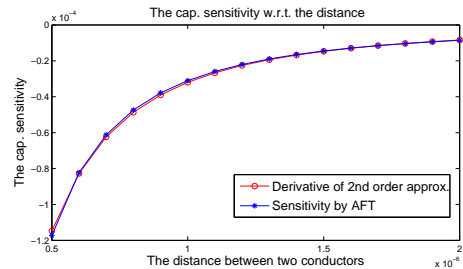


Figure 3: Simulation results w.r.t. d : $d = 0.5 - 2\mu\text{m}$.

We also conducted another similar experiment with t , the thickness of the conductors, instead of d as the geometric parameter. The system contains two conductors with a width $w = 2\mu\text{m}$ and a separation distance $d = 3\mu\text{m}$. The total number of panels is 2000. The average and the maximum differences between $\frac{\partial C}{\partial t}^A$ and $\frac{\partial C}{\partial t}^n$ are 5.36% and 5.74% respectively over the range of $t = 2\mu\text{m} - 5\mu\text{m}$.

Conclusion and Future Work

A new AFT-based algorithm is proposed for the calculation of capacitance sensitivity w.r.t. geometric variations for capacitance extraction considering process variability. This highly efficient algorithm requires no additional costly computation once the partial c -matrix is extracted. Although so far the experiments shown above only consider 2D interconnect structures, we believe the algorithm can be applied to 3D structures as well.

References

- [1] K. Agarwal, D. Sylvester, D. Blaauw, F. Liu, S. Nassif, and S. Vrudhula, “Variational delay metrics for interconnect timing analysis,” in *Proc. 41st Design Automation Conference*, pp. 381–384, 2004.
- [2] H. Kinzelbach, “Statistical variations of interconnect parasitics: Extraction and circuit simulation,” *Signal Propagation on Interconnects IEEE Workshop*, pp. 33–36, 2006.
- [3] A. Labun, “Rapid method to account for process variation in full-chip capacitance extraction,” *IEEE Trans. Computer-Aid Design*, vol. 23, no. 6, pp. 941–951, 2004.
- [4] B. Tellegen, “A general network theorem, with applications,” *Philips Research Report*, vol. 7, pp. 259–269, 1952.
- [5] P. Penfield, J. R. Spence, and S. Duinker, *Tellegen’s Theorem and Electrical Network*. M.I.T. Press, 1970.
- [6] D. Ioan, I. Munteanu, and G. Ciuprina, “Adjoint field technique applied in optimal design of a nonlinear inductor,” *IEEE Trans. Magn.*, vol. 34, no. 5, pp. 2849–2852, 1998.
- [7] N. Nikolova, J. Bandler, and M. Bakr, “Adjoint techniques for sensitivity analysis in high-frequency structure CAD,” *IEEE Trans. Microwave Theory Tech.*, vol. 52, no. 1, pp. 403–419, 2004.
- [8] E. J. Rothwell and M. J. Cloud, *Electromagnetics*. CRC Press, 2001.
- [9] M. Wentworth, Stuart, *Applied Electromagnetics: Early Transmission Lines Approach*. Wiley, 2007.
- [10] A. Ruehli, “Equivalent circuit models for three-dimensional multiconductor systems,” *IEEE Trans. Microwave Theory Tech.*, vol. 22, pp. 216–221, 1974.
- [11] *Space User’s Manual*. <http://www.space.tudelft.nl>.